

# Hollow nitrogen-doped carbon spheres as efficient and durable electrocatalysts for oxygen reduction†

 Jakkid Sanetuntikul,<sup>a</sup> Tao Hang<sup>\*b</sup> and Sangaraju Shanmugam<sup>\*a</sup>

 Cite this: *Chem. Commun.*, 2014, 50, 9473

 Received 7th May 2014,  
Accepted 14th June 2014

DOI: 10.1039/c4cc03437f

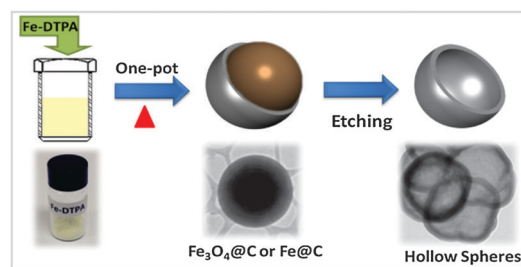
[www.rsc.org/chemcomm](http://www.rsc.org/chemcomm)

**Hollow nitrogen-doped carbon spheres (HNCSs) were prepared by a facile method as non-precious catalysts for the oxygen reduction reaction (ORR). The HNCS catalysts exhibited ORR activity comparable with a commercial Pt/C catalyst and superior stability in alkaline electrolyte medium.**

Proton exchange membrane fuel cells (PEMFCs) have been extensively studied over the last two decades and are still receiving tremendous interest as a promising power source for zero-emission electric vehicles due to their high-energy conversion efficiencies and a low level of air pollution.<sup>1</sup> Electrocatalysts play an important role in driving the fuel cell reactions. Generally Pt nanoparticles dispersed on high surface area carbon supports (Pt/C) and Pt-alloys with transition metals are used as major catalysts for fuel cells. Still, Pt/C is the most effective catalyst for the ORR. However, these catalysts impose a number of disadvantages such as high cost and a limited supply of Pt, which are the most technical limitations for the successful commercialization of fuel cell technology. Moreover, the poor ORR activity of Pt/C is also one of the major critical challenges for energy conversion efficiency of PEMFCs.<sup>2,3</sup> Meanwhile, many new types of Pt-based catalysts have been synthesized and explored as alternative catalysts to Pt/C and to reduce the Pt content. The design of high-performance cathode catalysts is essential to reduce the catalyst cost and improve the ORR activity and durability. Thus, the fabrication of highly active and durable non-precious catalysts is definitely preferable and has turned into a great challenge for today's fuel cell research community.<sup>4,5</sup>

Recently, nitrogen-doped carbon materials have received tremendous importance as non-precious electrodes, as the

incorporation of nitrogen into carbon frameworks can create active sites for oxygen adsorption and reduction. Various nitrogen-doped carbon materials, including carbon nanotubes (CNTs),<sup>6,7</sup> multi-wall carbon nanotube (MWCNTs),<sup>8,9</sup> mesoporous carbon,<sup>10</sup> graphene<sup>11,12</sup> and metal-organic framework (MOFs),<sup>13</sup> have been explored as alternative catalysts to Pt/C. However, the ORR activities of N-doped carbon materials are still less competitive compared to Pt. Therefore, the development of cost-effective and highly active ORR catalysts is required. Herein, we developed a simple and an easy method for the preparation of hollow nitrogen-doped carbon spheres (HNCSs) and explored as non-precious catalysts for the ORR. The fabrication of HNCS was accomplished by a facile and cost-effective route using dry-autoclaved iron(III) diethylenetriaminepentaacetate (Fe-DTPA) as a single precursor for carbon, nitrogen and iron. The reported method is straightforward, environmentally friendly, highly reproducible, solvent- and catalyst-free as well as easy to handle. The synthesis was carried out by pyrolysing the precursor at 700 °C and 900 °C with a heating rate of 10 °C min<sup>-1</sup> for 1 h under autogenic pressure resulting in Fe<sub>3</sub>O<sub>4</sub> and Fe<sup>0</sup> filled carbon spheres, respectively (Fig. S2–S4, ESI†). The as-synthesized products were stirred in concentrated HCl for 24 h at room temperature to remove the oxide core, and the carbons derived from Fe<sub>3</sub>O<sub>4</sub>@C and Fe@C were denoted as HNCS71 and HNCS91, respectively (Scheme 1). The acid treated products were washed



**Scheme 1** Pictorial representation of the fabrication of hollow nitrogen-doped carbon spheres.

<sup>a</sup> Department of Energy Systems Engineering, Daegu Gyeongbuk Institute of Science and Technology (DGIST), Daegu, 711-873, Republic of Korea.  
E-mail: sangarajus@dgist.ac.kr; Fax: +82 53 785 6409

<sup>b</sup> State Key Laboratory of Metal Matrix Composites, School of Material Science and Engineering, Shanghai JiaoTong University, Shanghai, 200240 P. R. China.  
E-mail: hangtao@sjtu.edu.cn

† Electronic supplementary information (ESI) available: Experimental details, additional SEM images and additional results. See DOI: 10.1039/c4cc03437f



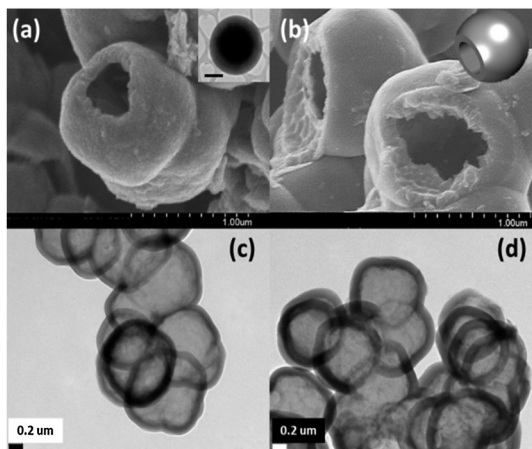


Fig. 1 FESEM images of (a) HNCs71 and (b) HNCs91, and TEM images of (c) HNCs71 and (d) HNCs91; inset in (a) shows a TEM image of a sphere before acid etching (scale bar: 1  $\mu\text{m}$ ), (b) shows a model of an open hollow sphere.

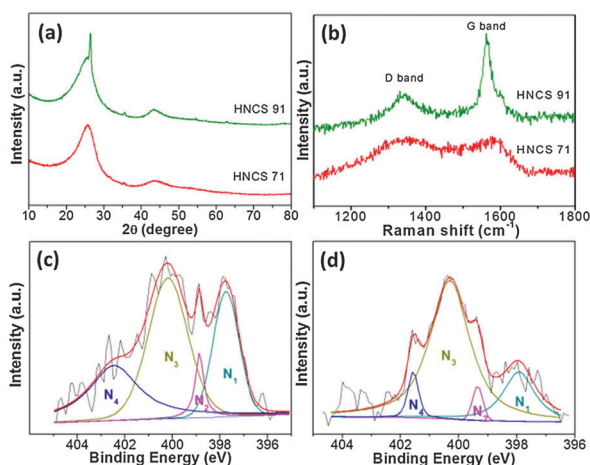


Fig. 2 (a) XRD patterns and (b) Raman spectra of HNCs and XPS N1s spectra of (c) HNCs71, and (d) HNCs91.

with copious water till the pH of aliquots became neutral, and then dried overnight in a vacuum oven.

Fig. 1a and b show the SEM images of HNCs71 and HNCs91 and reveal that after acid treatment, the products show a hollow sphere structure of carbon. The hollow sphere diameter is about 800 nm with a wall thickness of 100 nm and these spheres are free from oxide and metal cores, clearly evidenced by high-resolution TEM images (Fig. 1c and d). The X-ray diffraction patterns of HNCs71 and HNCs91 catalysts are shown in Fig. 2a. The HNCs91 catalyst showed a strong and sharp peak at  $27.1^\circ$  ( $2\theta$ ) indicating the formation of a highly ordered carbon structure, which is due to the higher temperature pyrolysis ( $900^\circ\text{C}$ ), whereas HNCs71 showed broad diffraction peaks at  $24.9^\circ$  and  $43.1^\circ$  ( $2\theta$ ) which correspond to the graphitic (002) and (101) hexagonal carbon structures, respectively.<sup>14</sup> XRD results further confirm that the oxide and metal cores were removed from the products but a small amount of iron was still present in carbon, which was clearly observed by STEM mapping analysis (Fig. S5, ESI†).

Fig. 2b shows the Raman spectra of HNCs71 and HNCs91 samples exhibiting two Raman bands centred at  $\sim 1360$  and  $\sim 1590\text{ cm}^{-1}$ , respectively, commonly identified as D- and G-bands of carbon. The D- and G-bands are ascribed to the disordered carbon ( $\text{sp}^3$ ) and ordered graphitic carbon ( $\text{sp}^2$ ), respectively. The nature of carbon present in HNCs can be identified by taking the integrated intensity ratio of D- and G-bands ( $I_D/I_G$ ).<sup>15</sup> A near-zero value of  $I_D/I_G$  indicates high crystallinity (well graphitized) while a value near one indicates existence of more defects in the carbon framework. The  $I_D/I_G$  values of HNCs71 and HNCs91 were 0.94 and 0.35, respectively. These values suggest that the HNCs91 sample exhibits a more ordered graphitic carbon structure than HNCs71, which is due to the higher temperature during the synthesis of the precursor and is in good agreement with XRD results.

The Brunauer–Emmett–Teller (BET) surface areas of the HNCs71 and HNCs91 samples were found to be 11.82 and 10.79  $\text{m}^2\text{ g}^{-1}$ , respectively. These results indicate that different pyrolysis temperatures have no effect on surface areas (Fig. S6, ESI†). The XPS survey spectra of the hollow carbon spheres revealed the presence of C, O, and N (Fig. S7, ESI†). The surface nitrogen content values of HNCs71 and HNCs91 samples measured by XPS were found to be 10.4 and 4.12 at%, respectively (Table S2, ESI†). The XPS high-resolution N1s spectra were deconvoluted into four peaks with binding energy (BE) values of 397.9, 399.4, 400.7, and  $\sim 402$  eV for HNCs71 and HNCs91 which can be assigned to the pyridinic-type,<sup>12,16</sup> benzenoid amine ( $-\text{NH}-$ )<sup>17</sup> or pyrrolic-type,<sup>6,18</sup> graphitic-type and oxidized-type<sup>12,18,19</sup> of nitrogen compounds, respectively (Fig. 2c and d). The HNCs71 catalyst showed a higher pyridinic-type nitrogen content (26.51%) than the HNCs91 (15.71%) catalyst. The pyridinic-nitrogen has an extra electron lone pair, which affects the conjugation of the nitrogen lone pair electrons on the nitrogen and hexagonal carbon  $\pi$ -system, and thus creates active sites for the ORR.<sup>6,12,18,20</sup> Furthermore, by the quantitative analyses of HNCs samples the ratio of doped-N to C (N/C ratio) of HNCs71 and HNCs91 was found to be 0.13% and 0.05%, respectively. The N/C ratio observed in XPS is in good agreement with the results obtained by the element analysis (Tables S2 and S3, ESI†).

The electrocatalytic oxygen reduction of hollow nitrogen-doped carbon spheres was studied by rotating disc electrode (RDE) experiments. A set of ORR polarization curves recorded from 400 to 2500 rpm in 0.1 M KOH solution at a scan rate 10  $\text{mV s}^{-1}$  are displayed in Fig. 3a. The results were compared with the ones obtained using the Pt/C catalyst (10% Pt/C, Johnson Matthew). The oxygen reduction onset potentials of HNCs71, HNCs91 and Pt/C catalysts were found to be 0.97, 0.88 and 1.02 V, respectively and the half-wave ( $E_{1/2}$ ) potentials were found to be 0.82, 0.69 and 0.85 for HNCs71, HNCs91 and Pt/C, respectively. The  $E_{1/2}$  of HNCs71 is 30 mV lower than that of the Pt/C catalyst and 130 mV higher than that of the HNCs91 catalyst (Fig. 3c). In addition, the HNCs71 catalyst showed a good diffusion-limited current suggesting better oxygen reduction activity. A well-defined diffusion-limited current density region of 0.3–0.7 V vs. RHE in RDE at different rotating speeds was used to calculate the number of electrons transferred during the ORR. For comparison, the ORR activity of various carbons was carried out and results are listed in Table S1 (ESI†). The HNCs71 catalyst showed a



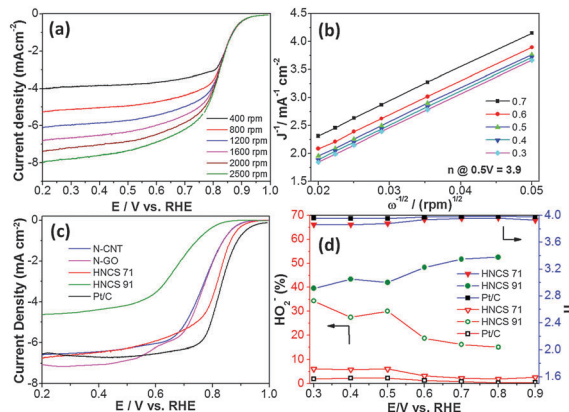


Fig. 3 (a) Polarization curves of HNCS71 in  $O_2$ -saturated at different rotation speeds, (b) corresponding Koutecky–Levich plots of HNCS71 at different electrode potentials, (c) LSVs of HNCS71, HNCS91, N-CNT, N-GO and Pt/C (10% Pt/C, Johnson Matthew) at 1600 rpm in  $O_2$ -saturated 0.1 M KOH, and (d) percentage of peroxide formation and the electron transfer number of these catalysts at different potentials, derived from RRDE experiments.

higher half-wave potential compared with nitrogen-doped graphene and nitrogen-doped carbon nanotubes, suggesting that the HNCS71 electrode can be a potential catalyst for the ORR in aq. 0.1 M KOH solution (Fig. 3c). The Koutecky–Levich (K–L) plots shown in Fig. 3b are derived from Fig. 3a and these plots show a good linearity and parallelism over the entire potential range, which indicates that the electron transfer number for the ORR was same even at high potentials.<sup>16</sup> The electron transfer number ( $n$ ) of HNCS71 and HNCS91 evaluated at 0.5 V vs. RHE was found to be 3.9 and 2.96, respectively, suggesting that the HNCS71 electrocatalyst exhibits a dominant four-electron oxygen reduction process. According to these results, HNCS71 exhibits a higher ORR activity than HNCS91, which can be attributed to the higher content of active sites. Especially, the HNCS71 catalyst exhibits more pyridinic-type nitrogen, which is bonded to two carbon atoms in the carbon plane with a lone pair of electrons associated with the formation of Fe–N<sub>x</sub> active sites in the carbon framework, and enhance the ORR activity.<sup>13,20</sup> It is also consistent with the N/C ratio obtained from the element analysis and XPS results (Tables S2 and S3, ESI†) reveal that the HNCS71 catalyst exhibits a higher total doped-nitrogen content in the carbon network (N/C ratio), which plays an important role in improving the ORR onset and the  $E_{1/2}$  potential. Dodelet and co-workers proposed metal cations coordinated by pyridinic-nitrogen atoms at defects of carbon as active ORR sites.<sup>13,20</sup> To further confirm the ORR results obtained from the RDE, we carried out the rotating-ring disk electrode (RRDE) measurements to evaluate the formation of peroxide species ( $HO_2^-$ ) during the ORR process. From the ring and disk currents recorded at 1600 rpm in 0.1 M KOH with  $O_2$ -saturated over HNCS71, HNCS91 and Pt/C catalysts as shown in Fig. S8, ESI† it can be seen that the ring and disk currents of HNCS71 are almost comparable with the currents observed for a commercial Pt/C catalyst. The percentage of  $HO_2^-$  and the number of electrons transferred ( $n$ ) derived from RRDE experiments are presented in Fig. 3d. The percentage of peroxide ( $HO_2^-$ ) formation for the HNCS71 catalyst was below

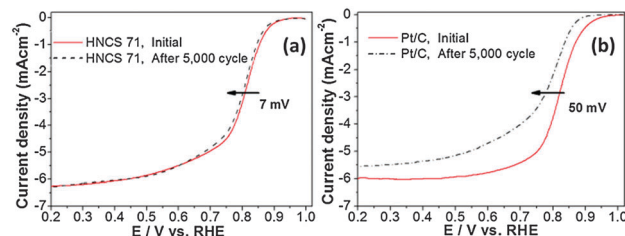


Fig. 4 Polarization curves measured during cycling durability tests at 1600 rpm in  $O_2$ -saturated 0.1 M KOH (cycling tests were carried out in a potential window of 0.6–1.0 V vs. RHE with 50 mV s<sup>−1</sup>).

6% over a potential range of 0.3–0.9 V, whereas the HNCS91 catalyst produced a large amount of peroxide (20–35%) over the potential range of 0.3–0.8 V. The electron transfer number was found to be 3.9 for HNCS71 and about 2.8–3.3 for HNCS91, which is in good agreement with the electron transfer number observed from RDE experiments and it clearly illustrated that the HNCS71 catalyst can efficiently reduce oxygen via a 4-electron reduction pathway in alkaline medium.

The electrochemical stability of the non-precious catalyst was evaluated by performing repeated potentiodynamic cycling durability tests for 5000 cycles in  $O_2$ -saturated 0.1 M KOH solution with a potential window of 0.6–1.0 V and at a scan rate of 50 mV s<sup>−1</sup>. It was found that, after 5000 cycles, a 7 mV negative shift of  $E_{1/2}$  was observed for HNCS71, whereas a 50 mV negative shift was observed for the Pt/C catalyst (Fig. 4). Furthermore, no change in the current density of HNCS71 upon cycling indicated that surface properties were maintained during potential cycling tests.<sup>18,21,22</sup> On the basis of these studies, the HNCS71 catalyst showed better electrochemical stability than the Pt/C catalyst.

In summary, we have successfully fabricated a new kind of non-precious catalyst, a hollow nitrogen-doped carbon sphere as a cathode catalyst through a simple and scalable approach. The HNCS71 catalyst exhibited ORR activity comparable with that of a commercial Pt/C catalyst and better stability in an alkaline medium. These results demonstrate that the type of nitrogen doping and tuning the nitrogen content in the carbon framework could be a potential choice for the development of low-cost, highly active ORR catalysts for fuel cell applications.

This work was financially supported by the DGIST R&D Program of the Ministry of Education, Science and Technology of Korea (14-BD-01).

## Notes and references

- M. K. Debe, *Nature*, 2012, **486**, 43–51.
- C.-L. Sun, L.-C. Chen, M.-C. Su, L.-S. Hong, O. Chyan, C.-Y. Hsu, K.-H. Chen, T.-F. Chang and L. Chang, *Chem. Mater.*, 2005, **17**, 3749.
- H. A. Gasteiger and N. M. Marković, *Science*, 2009, **324**, 48–49.
- F. Jaouen, E. Proietti, M. Lefèvre, R. Chenitz, J.-P. Dodelet, G. Wu, H. T. Chung, C. M. Johnston and P. Zelenay, *Energy Environ. Sci.*, 2011, **4**, 114–130.
- Z. Chen, D. Higgins, A. Yu, L. Zhang and J. Zhang, *Energy Environ. Sci.*, 2011, **4**, 3167–3192.
- H. T. Chung, J. H. Won and P. Zelenay, *Nat. Commun.*, 2013, **4**, 1–5.
- K. Gong, F. Du, Z. Xia, M. Durstock and L. Dai, *Science*, 2009, **323**, 760–764.
- I. Kruusenberg, L. Matisen, Q. Shah, A. M. Kannan and K. Tammeveski, *Int. J. Hydrogen Energy*, 2012, **37**, 4406–4412.

- 9 T. Maiyalagan and B. Viswanathan, *Mater. Chem. Phys.*, 2005, **93**, 291.
- 10 W. Yang, T.-P. Feller and M. Antonietti, *J. Am. Chem. Soc.*, 2011, **133**, 206–209.
- 11 L. Qu, Y. Liu, J.-B. Baek and L. Dai, *ACS Nano*, 2010, **4**, 1321–1326.
- 12 H. Peng, Z. Mo, S. Liao, H. Liang, L. Yang, F. Luo, H. Song, Y. Zhong and B. Zhang, *Sci. Rep.*, 2013, **3**, 1–7.
- 13 E. Proietti, F. Jaouen, M. Lefèvre, N. Larouche, J. Tian, J. Herranz and J.-P. Dodelet, *Nat. Commun.*, 2011, **2**, 1–9.
- 14 H. Jin, H. Zhang, H. Zhong and J. Zhang, *Energy Environ. Sci.*, 2011, **4**, 3389–3394.
- 15 X.-Y. Yan, X.-L. Tong, Y.-F. Zhang, X.-D. Han, Y.-Y. Wang, G.-Q. Jin, Y. Qin and X.-Y. Guo, *Chem. Commun.*, 2012, **48**, 1892–1894.
- 16 S. Shanmugam and T. Osaka, *Chem. Commun.*, 2011, **47**, 4463–4465.
- 17 F. G. Souza Jr, P. Richa, A. De Siervo, G. E. Oliveira, C. Pinto and C. H. M. Rodrigues, *Macromol. Mater. Eng.*, 2008, **239**, 675–683.
- 18 C. V. Rao, C. R. Cabrera and Y. Ishikawa, *J. Phys. Chem. Lett.*, 2010, **1**, 2622–2627.
- 19 D. Choudhury, B. Das, D. D. Sarma and C. N. R. Rao, *Chem. Phys. Lett.*, 2010, **497**, 66–69.
- 20 M. Lefèvre, E. Proietti, F. Jaouen and J.-P. Dodelet, *Science*, 2009, **324**, 71–74.
- 21 Y. Li, W. Zhou, H. Wang, L. Xie, Y. Liang, F. Wei, J.-C. Idrobo, S. J. Pennycook and H. Dai, *Nat. Nanotechnol.*, 2012, **7**, 394–400.
- 22 G. Wu, K. L. More, C. M. Johnston and P. Zelenay, *Science*, 2011, **332**, 443–447.

